Tikrit Journal of Engineering Sciences (2025); 32(3): 1939
DOI: http://doi.org/10.25130/tjes.32.3.30

IRAQI Academic Scientific Journals

ISSN: 1813-162X (Print); 2312-7589 (Online)
Tikrit Journal of Engineering Sciences
available online at: http://www.tj-es.com

TJES Tikrit Journal of Engineering Sciences

Investigation of Wall Shape and Immersed Body Effect on Two Phases (Solid - liquid) Fluidized Bed

Huda Ridha *
Veterinary Medicine College, Wasit University, Wasit, Iraq.

Keywords:
Ansys Fluent; Computational fluid dynamics; Immersed tube; Multiphase; SolidWorks.

Highlights:

- *Wavy walls in a fluidized bed had better fluidization.*
- *Wavy walls, fluidized bed with immersed bodies, had more fluidization.*
- *Fluidization head increased by raising the inlet velocity and the initial head.*

ARTICLE INFO
Article history:

Received	23 Dec. 2023
Received in revised form	08 Feb. 2024
Accepted	20 Sep. 2024
Final Proofreading	20 Aug. 2025
Available online	28 Aug. 2025

Citation: Ridha H. **Investigation of Wall Shape and Immersed Body Effect on Two Phases (Solid - liquid) Fluidized Bed**. *Tikrit Journal of Engineering Sciences* 2025; **32**(3): 1939.
http://doi.org/10.25130/tjes.32.3.30

Corresponding author:
Huda Ridha
Veterinary Medicine College, Wasit University, Wasit, Iraq.

Abstract: The fluidized bed was commonly investigated with the walls of the test section being straight walls. The difference in this investigation is that the walls of the fluidized bed were taken as sine waves. The investigations were performed numerically. The SolidWorks software program was used to create the geometry, while the Ansys Fluent software program was used to perform the simulations. The computational fluid dynamics model was validated using the experimental and the numerical results from other research; it was also validated using the fluidized bed equation for velocity. The velocity of the flowing fluid was changed four times (0.15 m/s, 0.25 m/s, 0.35 m/s, and 0.45 m/s), while the initial height of the particles was altered two times (0.15 m and 0.25 m). Another geometry was created for the fluidized bed, which contained three holes that worked as immersed bodies. The results showed that the average pressure of the fluidized bed increased with the velocity of the working fluid. For a 0.15 m/s water velocity, the pressure was 9 kPa. As the water velocity was raised to 0.45 m/s, the pressure elevated to 13 kPa. Moreover, increasing the velocity of the working fluid led to an increase in the fluidization head. It was also shown that the wall shape created more turbulence and circulation in the fluidization process than the normal straight walls.

دراسة شكل الجدار وتأثير الجسم المغمور على انبوب التمييع للطورين (الصلب - السائل)

هدى رضا
كلية الطب البيطري / جامعة واسط / واسط - العراق.

الخلاصة
عادة ما يتم فحص الانبوب المميع بجدران أنبوب الاختبار التي كانت عبارة عن جدران ضيقة. الفرق في هذا البحث هو أن جدران الانبوب المميع اتخذت على شكل الدالة السينية المتموجة. تم إجراء البحث عدديا، وتم استخدام برنامج SolidWorks لإنشاء الشكل الهندسي، في حين تم استخدام برنامج Ansys Fluent لإجراء عمليات المحاكاة. تم التحقق من صحة النموذج الديناميكي للموائع الحسابية باستخدام النتائج التجريبية والعددية من أبحاث أخرى، كما تم التحقق من صحته باستخدام معادلة الطبقة المميعة للسرعة. تم تغيير سرعة مائع العمل أربع مرات (٠,١٥، ٠,٢٥، ٠,٣٥، ٠,٤٥) بينما تم تغيير الرأس الأولي للجزيئات مرتين (٠,١٥، ٠,٢٥). تم إنشاء هندسة أخرى للطبقة المميعة التي تحتوي على ثلاثة ثقوب تعمل كأجسام مغمورة. أظهرت النتائج أن متوسط ضغط الطبقة المميعة يزداد مع زيادة سرعة المائع العامل. علاوة على ذلك، أدت زيادة سرعة المائع العامل إلى زيادة رأس التميع. كما تبين أن شكل الجدران خلق المزيد من الاضطراب والتدوير في عملية التميع مقارنة بالجدران المستقيمة العادية.

الكلمات الدالة: Ansys Fluent، ديناميكا الموائع الحسابية، الأنبوب المغمور، متعدد الأطوار، SolidWorks.

1.INTRODUCTION

The procedure of fluidization involves altering the solid elements' behavior with the help of liquid or gas flow into a fluid-like state. The fluid of fluidization flows through the bed in an upward direction, while the particles are gathered in a bed maintained by a punctured plate. The flowing fluid is supposed to be distributed uniformly through the bed. The bed will reach a fluid-like state, with the particles being aggregated into a form, as the velocity of the flowing fluid becomes the fluidization velocity [1]. The technology of the fluidized bed is universally used in production industries, for instance, environmental protection, chemical engineering, pharmaceutical, and energy production. This importance makes the technology of fluidized bed constantly upgraded to meet the new society's requirements. One of the hot spot developments of the fluidized bed is the Microwave-assisted fluidized bed. Aerodynamic agitations are delivered with the fluidization process, which can be utilized for uniformly heating with the particles being stirred in the heated zones uninterruptedly, and with the fluid as a medium, making it less vulnerable to thermal runaway. A developed technology, such as the technology of the fluidized bed, has found its place in the world in metal ore processing, chemical deposition vapor process, drying process, and power generation [2, 3]. Large particles will either sink or float in a solid-liquid fluidized bed according to their density because of the like-liquid properties in the fluidized bed. Bed density was investigated by Refs. [4-7], a low density consisting of a single particle was noticed at the bottom region of the fluidized bed. Meanwhile, there was constant density in the upper region of the fluidized bed. It was also noticed that a high fluid velocity will not produce a constant density for the fluidized bed as a function of height. Chemical looping processes are generally used in a bubbling fluidized bed as the fuel reactor. A bubbling fluidized bed was investigated by [8-10]. Bubble energy and the maximum bubble size were reduced for each chamber due to the height/diameter ratio being decreased in each compartment by inserting the baffles in the bed. Some researchers often use computational fluid dynamics (CFD) and/or discrete element method (DEM) to numerically investigate fluidized beds [11-15], either by using the Euler-Euler-based model or the Eulerian-Lagrangian-based model. The fluidized bed performance results were similar whether they resulted from the two-fluid model (TFM) and/or from the CFD-DEM model. One of the fluidized bed features that affects the fluidization process is the inlet flow configuration. Tawfik et al. [16] investigated different configurations for inlet flow. It was observed that the particles moved upwardly at the center of the bed and downwardly near the walls when the lateral nozzle was located in the top part of the bed. When the location of the lateral nozzle was in the middle part of the bed, the movement was in reverse. The reaction efficiency and the relative velocity of fluid-solid can be improved further with the bidirectional fluidized bed compared to the traditional upward fluidized bed. One of the industrial processes that uses fluidized beds is the heating process. The hydrodynamic behaviors of the fluidized beds make it a particularly suitable choice for heat transfer, which is why several researchers have studied the fluidized bed as a thermal energy system for heat transfer, heat absorbers, and heat exchangers [17-21]. It was found that the bubbling fluidized bed showed better heat transfer performance than the turbulent fluidized bed. An external electrical field was proposed in a two-dimensional fluidized bed [22]. It was used to investigate the behavior of tribo-charging. A multi-stage fluidized bed was studied to investigate the process of mass transfer with a shallow fluidized bed [23]. The mass transfer was studied with the help of a phenomenological model. Gasification process and waste pyrolysis

process are usually performed with the help of fluidized bed reactors due to their efficiency in distributing temperature and mixing characteristics. Nevertheless, all this cannot be done when the system contains lumps. The lumps' heat transfer coefficients, dispersion coefficients, and the segregation behavior during the operation, and how they are affected by the physical and variable properties, were investigated [24]. A comparison was made between a square fluidized bed and a circular fluidized bed utilizing different solid holdups and pressure drops [25]. The characteristics of solid drying were enhanced within the fluidized bed using mechanical vibration, which improved the contacting of solid and fluid [26, 27]. The high coefficient of heat transfer among the immersed bodies or the wall in the fluidized bed makes it an effective way in the industrial processes that require heat transfer, such as fluidized bed combustion, reactors, and drying. Fluidized bed with different forms of immersed subjects was investigated by [28-30]. The heat transfer performance was found to be enhanced by the presence of bodies within the fluidized bed, such as horizontal and vertical tubes and fins. The purpose of this paper is to investigate the fluidized bed with wavy walls rather than a straight one. The effect of inserting immersed bodies on the flow distribution was also investigated. The other difference is that the material used for the solid particles was heavier than the other investigated materials.

2.NUMERICAL INVESTIGATION

The numerical investigations of this paper were performed using SolidWorks 2018 and Ansys Fluent 20. The model geometry was generated with SolidWorks using sine waves for both sides of the test pipe, which was used as a fluidized bed. Figure 1 (a) shows the fluidized bed two-dimensional geometry without the immersed bodies. Figure 1 (b) shows the fluidized bed two-dimensional geometry with the immersed bodies. The model is a two-dimensional model with a width of the fluidized bed set as 0.15 m, while the height of the fluidized bed was set as 1 m. A quadrilateral mesh was generated with Ansys Fluent meshing. Maximum mesh size was set as 2.5 mm while minimum mesh size was set as 0.3 mm, which produced 25312 elements and 25787 nodes for the geometry without the immersed bodies and 25090 elements and 25634 nodes for the geometry with the immersed bodies. Figure 2 shows the mesh in the fluidized bed with the immersed bodies. Figure 3 shows the grid independence test. Eulerian- Eulerian multiphase model was utilized for the simulation. Water was set as the working fluid, while 1.5 mm diameter stainless steel with 8000 kg/m^3 was set as the solid particles. The turbulent model was set as the k-epsilon model, while the drag modification between water and solid particles was set as Morsi-Alexander. The model was investigated as a transient model with 0.001 seconds as the time step size and 20 iterations per time step. Generally, the number of time steps was taken as 1400. For the boundary conditions, the base of the test section was set as the inlet velocity for water, which was changed four times (0.15, 0.25, 0.35, and 0.45 m/s). While the top of the test section was set as the outlet pressure. The initial head for the solid particles was set as 0.15 m for all water velocities, and then changed to 0.25 m for all water velocities. The operating pressure was set as 101325 Pa. While the operating gravity was set as -9.81 m/s^2. The residuals were set as 10-6 for continuity, velocities, and volume fraction. Pressure under relaxation was set as 0.5, while momentum and volume fraction under relaxation were set as 0.2 and 0.5, respectively. Table 1 shows the simulation variables used in the present investigations.

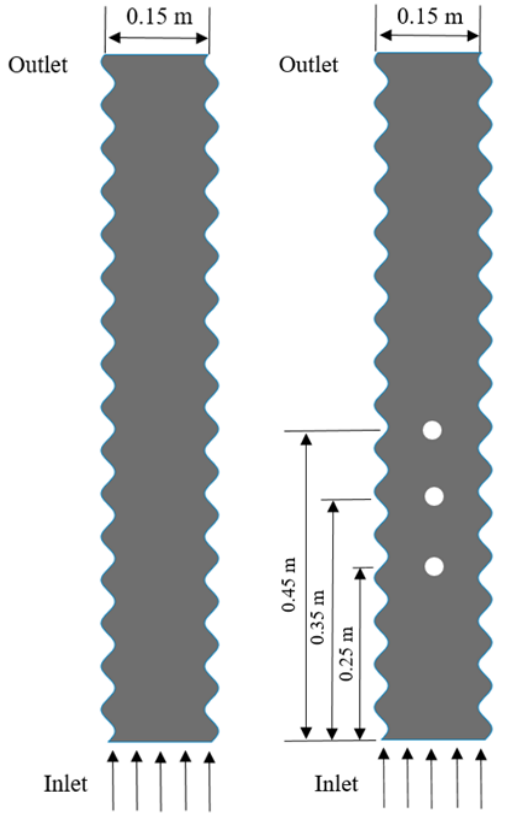

(a) without Immersed Bodies. **(b)** with Immersed Bodies.

Fig. 1 Model Geometry.

Table 1 Simulation Variables.

Properties	Value
Solid phase density	8000 kg/m^3
Maximum mesh size	2.5 mm
Solid volume fraction	0.76
Solid particles diameter	1.5 mm
Head of solid particles	0.15 m and 0.25 m
Velocity of water	0.15, 0.25, 0.35, and 0.45 m/s
Time step size	0.001 second
Water viscosity	0.001003 kg/m.s
Water density	998.2 kg/m^3
Number of time steps	1400
Factor of under-relaxation for pressure	0.5
factor of under-relaxation for volume fraction	0.5
Factor of under-relaxation for momentum	0.2

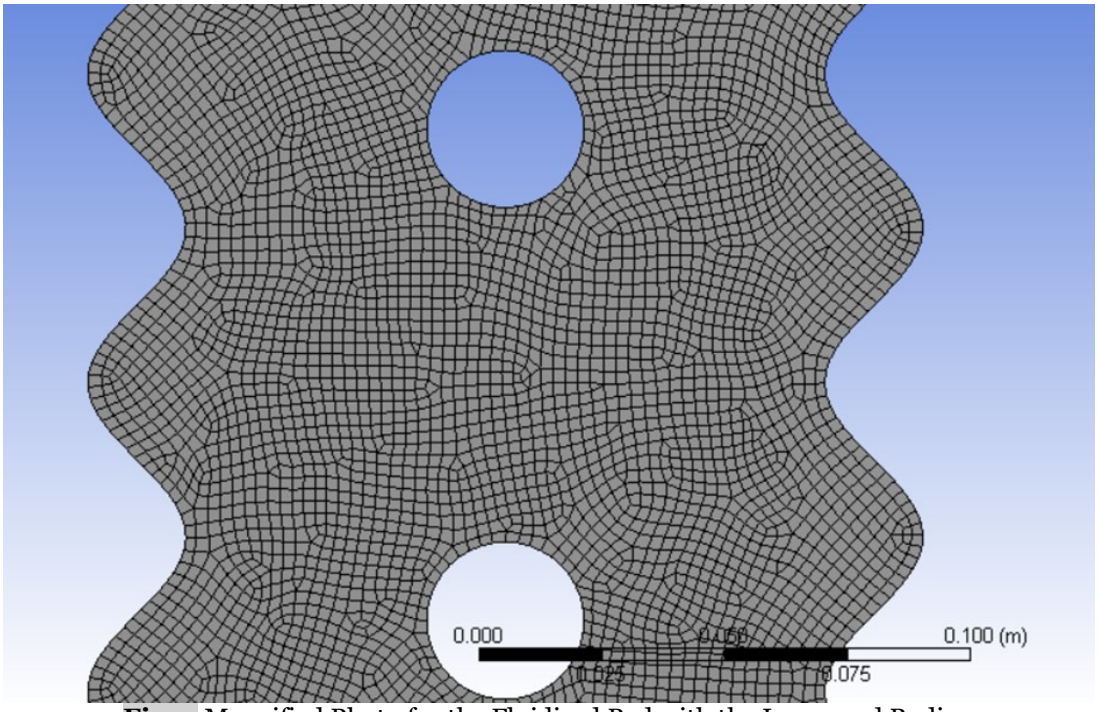

Fig. 2 Magnified Photo for the Fluidized Bed with the Immersed Bodies.

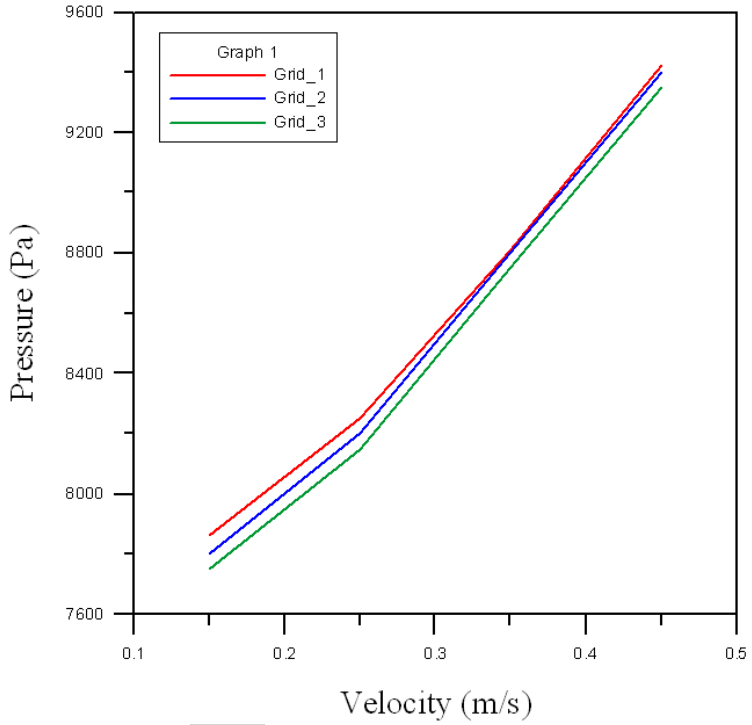

Fig. 3 Grid Independence Study.

2.1.The Governing Equations

The Eulerian multiphase model generally uses the equations of momentum conservation and mass conservation. The momentum conservation equation can be written in its general form as:

$$\frac{\partial}{\partial t}(\alpha_q \rho_q \vec{v}_q) + \nabla.(\alpha_q \rho_q \vec{v}_q \vec{v}_q) = -\alpha_q \nabla p + \nabla.\bar{\bar{\tau}}_q + \alpha_q \rho_q \vec{g} + \sum_{p=1}^{n} (\vec{R}_{pq} + \dot{m}_{pq} \vec{v}_{pq} - \dot{m}_{qp} \vec{v}_{qp}) + (\vec{F}_q + \vec{F}_{lift,q} + \vec{F}_{vm,q}) \quad \textbf{(1)}$$

where $\bar{\bar{\tau}}_q$ is the stress-strain tensor.

$$\bar{\bar{\tau}}_q = \alpha_q \mu_q (\nabla \vec{v}_q + \nabla \vec{v}^{T}_{q}) + \alpha_q (\lambda_q - \frac{2}{3}\mu_q) \nabla.\vec{v}_q \bar{\bar{I}} \quad \textbf{(2)}$$

q represents the phase in all equations

The mass conservation equation can be written in its general form as:

$$\frac{\partial}{\partial t}(\alpha_q \rho_q) + \nabla.(\alpha_q \rho_q \vec{v}_q) = \sum_{p=1}^{n} \dot{m}_{pq} - \dot{m}_{qp}) + S_q \quad \textbf{(3)}$$

The source term, S_q, is zero by default, or it can be a set constant value or defined by the user.

2.2.Model Validation

The experimental and the numerical results from Al-Turaihi and Oleiwi [31] were used to validate the present model. A two-dimensional structure was used as a test section (1 m× 0.0254 m). Granular flow model (GFM), which is, in other words, the Eulerian approach, was used for the simulations. Based on the Reynolds number, a turbulent configuration was chosen for the model. Figure 4 shows a contrast between the experimental results and the validated results. Three diverse values of initial bed height were revealed at each value of water flow rate and for three formats of water flow rate. As the water flow rate increased, the expansion of the bed increased. The pressure of the bed increased when the volume flow rate elevated due to the increase in the mixture density.

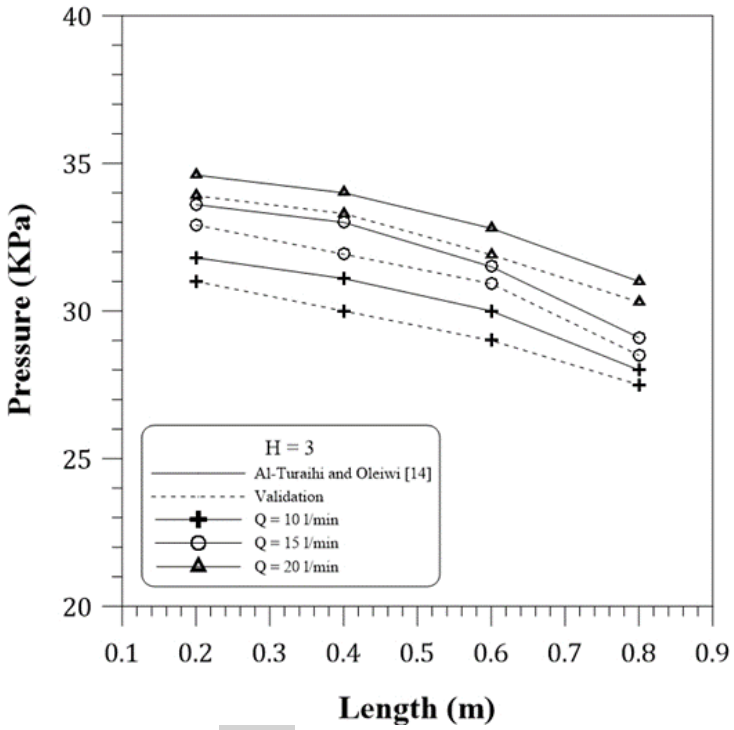

Fig. 4 Model Validation.

3.RESULTS AND DISCUSSION

The walls of the fluidized bed in this paper were taken as sine waves instead of the straight line walls that were used in previous work on the fluidized bed. Figure 5 shows the difference in the flow characteristics from the start of the fluidization process between the straight walls and the wavy walls. The water velocity and the initial particles head were the same for both cases, i.e., 0.25 m/s and 0.15 m, respectively. The time was taken from 0.2 seconds after the fluidization started to 1 second. Figure 5 shows that the fluidization of the solid particles started earlier for the fluidized bed with wavy walls than for the fluidized bed with straight walls. As shown in Fig. 5, at 0.8 seconds, the fluidized bed with wavy walls was fully fluidized. Whereas the fluidized bed with straight walls was not completely fluidized even after 1 second, i.e., the wavy walls reduced the time required to reach a fully fluidized state.

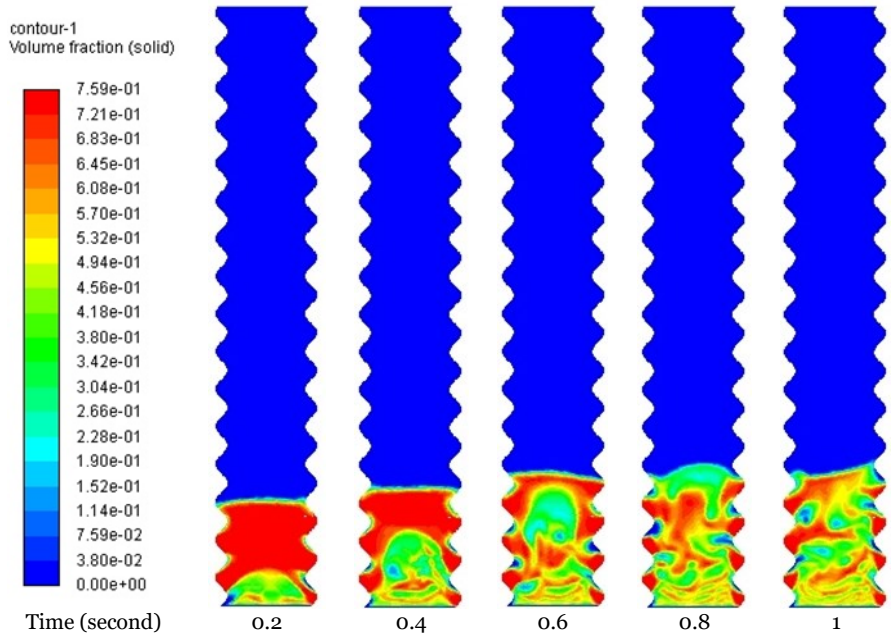

Fig. 5 Effect of Wall Shape on the Flow Characteristics at Water Velocity of 0.25 m/s and Initial Solid Particles Head of 0.15 m.

Figures 6 and 7 show the impact of water velocity on the head of the fluidization after 1.4 seconds from the initial state. The velocity of water changed from 0.15 m/s to 0.45 m/s. Every time the water velocity increased, the head of fluidization rose. Figure 6 shows the impact of water velocity at an initial solid particles head of 0.15 m, at 0.15 m/s water velocity. The head of fluidization was unchanged from the initial state, although there was movement in the solid particles. For a water velocity of 0.25 m/s, the head of the fluidization started to increase gradually. Reaching a water velocity of 0.45 m/s, the head of fluidization became almost twice the initial solid head, agreeing with the finding of [32], where they investigated the minimum fluidization velocity as a function of the bed head to the bed diameter. The same behavior was observed at 0.25 initial solid particles head, tested with the same values of water velocity, as shown in Fig. 7. Also, more fluidization was noticed as the water velocity increased for both cases of initial solid head. At 0.35 m/s and 0.45 m/s, the solid particles became more separated than at 0.25 m/s and 0.15 m/s, as shown in Figs. 6 and 7, due to the increase in the turbulence in the fluidized bed.

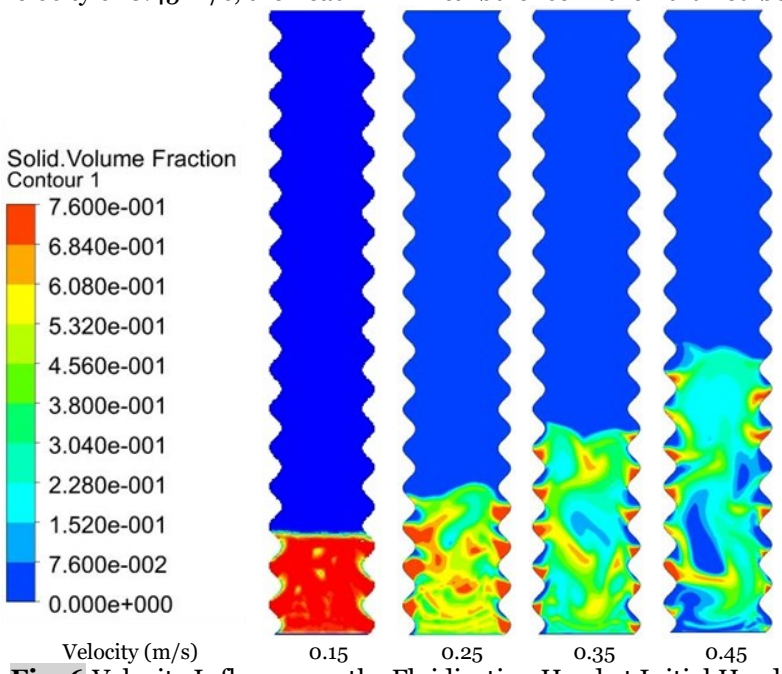

Fig. 6 Velocity Influence on the Fluidization Head at Initial Head of 0.15 m.

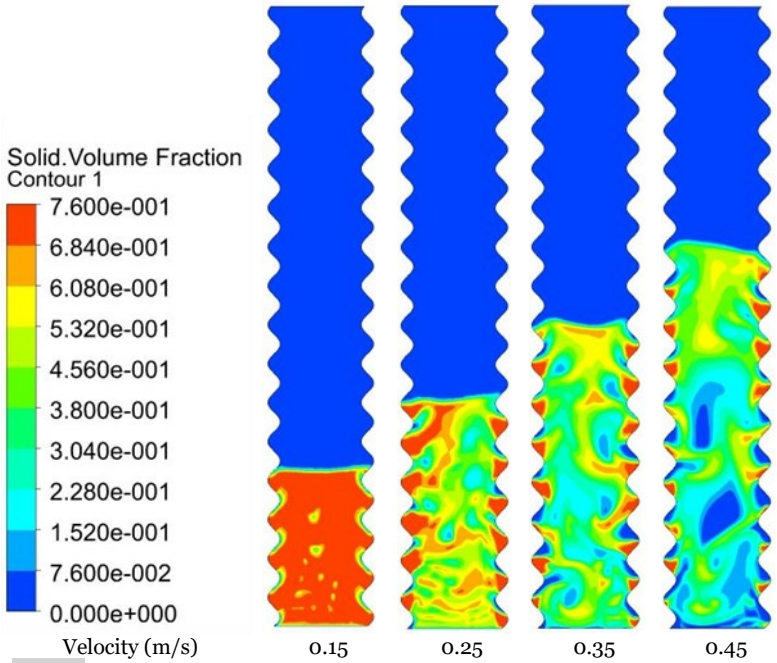

Fig. 7 Velocity Influence on the Fluidization Head at Initial Head of 0.25 m.

When the flow velocity continuously increased through a packed bed, the pressure drop across the bed continued to increase. The bed pressure drop became equivalent to the bed weight when the flow rate reached a specific value; this point is the fluidization point. The minimum fluidization velocity was the equivalent superficial velocity across the bed. To estimate the minimum fluidizing velocity, Eq. 4 can be used [33]:

$$U_{mf} = \frac{gy\,(r_p - r)D_p^{\,2}e_m^{\,3}}{150m(1 - e_m)} \qquad \textbf{(4)}$$

where is the dimensionless parameter (0.5-1), is the dimensionless parameter that represents the void fraction where the fluidization velocity is at its minimum value, is the mean particle diameter, g is the gravitational constant, μ is the fluid viscosity, is the particle density, and is the fluid density. Applying Eq. 4 with a 0.5 minimum void fraction, and y=1.

$$U_{mf} = \frac{9.81(8000 - 998.2)(1.5' 10^{-3})^2(0.5)^3}{150' 0.001003(1 - 0.5)}$$

$$U_{mf} = 0.25m/s$$

It is shown from Figs. 6 and 7 that the fluidization process did not commence at a velocity of 0.15 m/s. However, the fluidization process started as the velocity of water increased from 0.15 m/s to 0.25 m/s, which is in perfect lining with the simple formal of the minimum fluidization velocity, Eq. 4. The results of having an immersed body inside the fluidized bed as a circular shape with 0.032 m diameter are shown in Figs. 8 and 9, close to the behavior found by [34]. The results showed that having immersed bodies inside the fluidized bed insignificantly impacted the fluidization height when comparing the results from Figs. 6 and 7 with the results from Figs. 8 and 9. However, the flow circulation and turbulence were significantly improved as the immersed bodies were added to the fluidized bed geometry. Having immersed bodies in the fluidized bed acted as an obstacle for the fluidized particles. The obstacle caused the particles to collide more frequently, creating a circular motion within the bed. Figure 10 shows the solid particles velocity vectors for the straight fluidized bed, the wavy fluidized bed, and the wavy fluidized bed with immersed bodies. It shows that the circulation of particles was enhanced when the walls of the fluidized bed were shaped as a sine wave. However, it was significantly enhanced by adding these three circular-shaped immersed bodies. The average pressure of the fluidized bed is shown in Fig. 11 with respect to the water velocity. Raising the water velocity entering the fluidized bed increased the pressure inside the bed for both the initial solid head tested and for the fluidized bed when the immersed bodies were included. The drag force of the water moving in the upward direction was offset by the particle's gravitational force. The decrease in fluidized bed pressure was proportional to the water velocity, consistent with the results of [35, 36]. The pressure values were calculated at 1.4 seconds after the simulation started. Figure 11 also shows the effect of the initial solid head on the average pressure inside the fluidized bed. Having a large amount of solid particles inside the fluidized bed led to a higher pressure than a smaller amount. Figure 11 also shows that having immersed bodies inside the fluidized bed led to a reduction in the overall average pressure inside the fluidized bed.

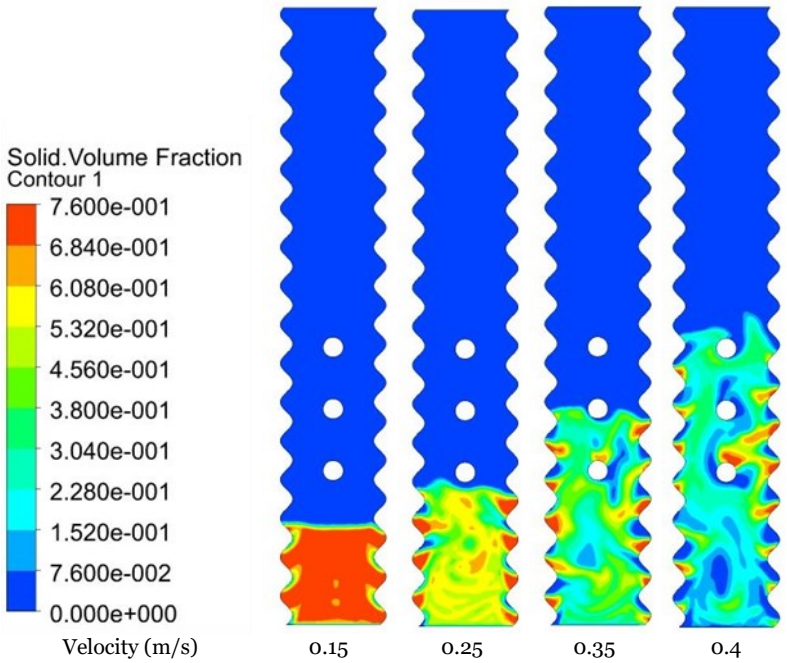

Fig. 8 Velocity and Immersed Bodies Influence on the Fluidization Head at 0.15 m Initial Head.

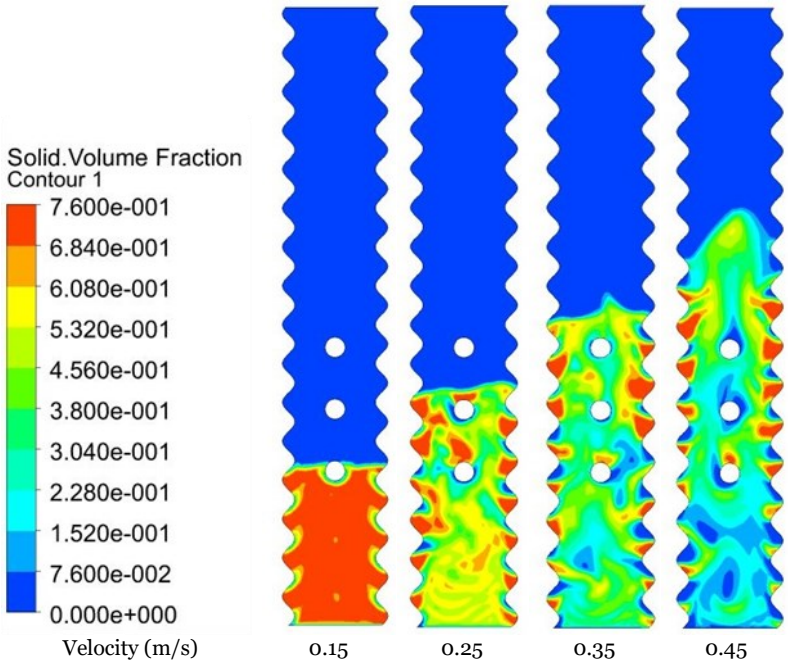

Fig. 9 Effect of Velocity and Immersed Bodies on the Fluidization Head at 0.25 m Initial Head.

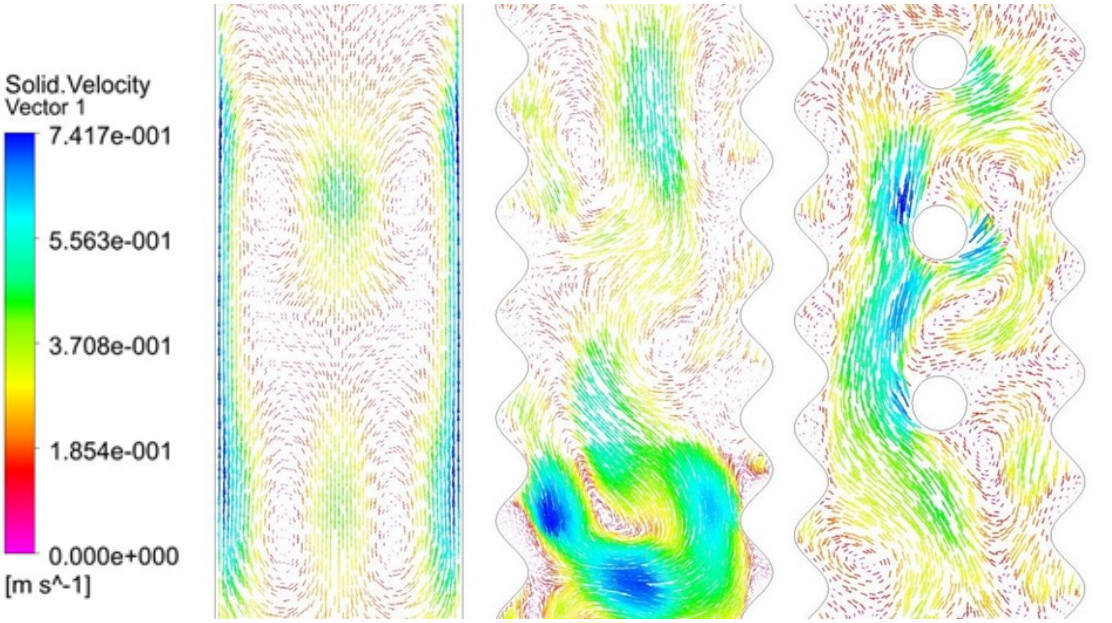

Fig. 10 Particle Velocity Vectors for Velocity of 0.45 m/s and Initial Particles Head of 0.15 m.

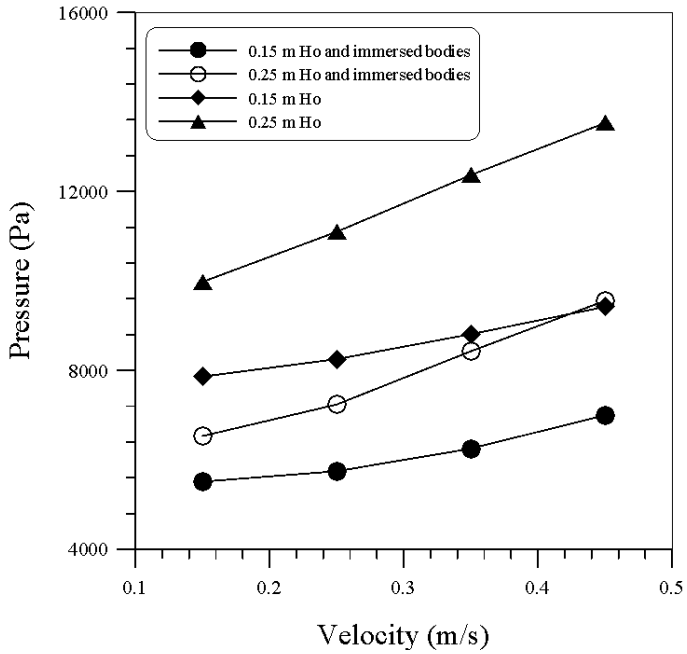

Fig. 11 Effect of Velocity on the Pressure of the Fluidized Bed.

The average pressure at different distances from the inlet of the fluidized bed is shown in Fig. 12, for 0.15 m and 0.25 m initial solid particles head. Figure 12 shows that the pressure at the low partition of the fluidized bed was at its highest value compared to its top partition, consistent with the findings of [37]. The value of pressure was taken 1.4 seconds after the start of the simulations at a water velocity of 0.45 m/s. The solid particles were initially located at the base of the fluidized bed, and by the force of the flowing water, they were transferred through the pipe; therefore, the pressure at the base of the fluidized bed was high. It started to decrease in the vertical direction of the fluidized bed. Figure 13 shows the velocity of the solid particles at various locations through the fluidized bed. The solid particles acquired velocity as they were forced to move by the flow of water. The values of solid particles' velocity were taken after 1.4 seconds from the start of the simulations at a water velocity of 0.45 m/s. The particles do not acquire the exact value of velocity because they keep colliding with each other, increasing or reducing the particles' velocity, as shown in Fig. 13. However, Fig. 13 shows that the solid particles' velocity was almost the same at the middle of the fluidization head.

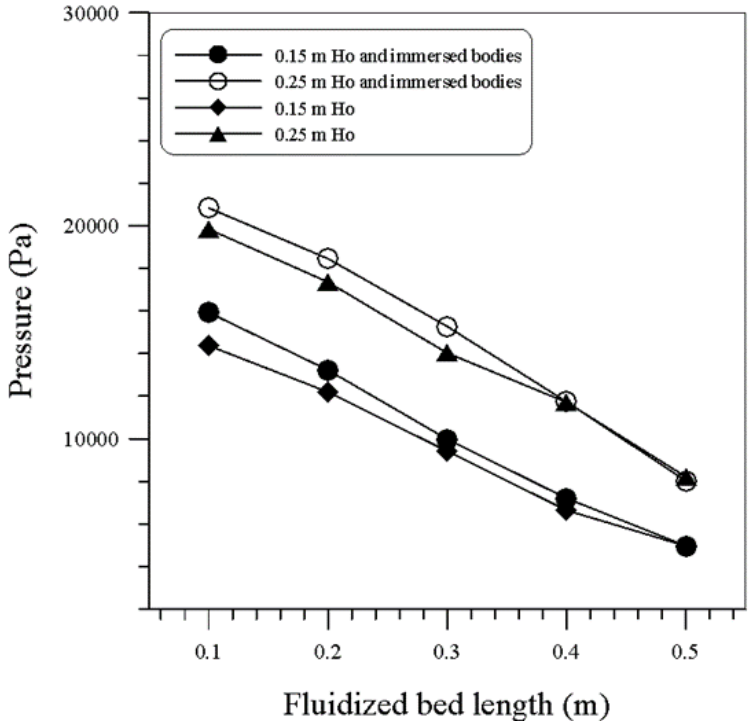

Fig. 12 Pressure Through the Fluidized Bed.

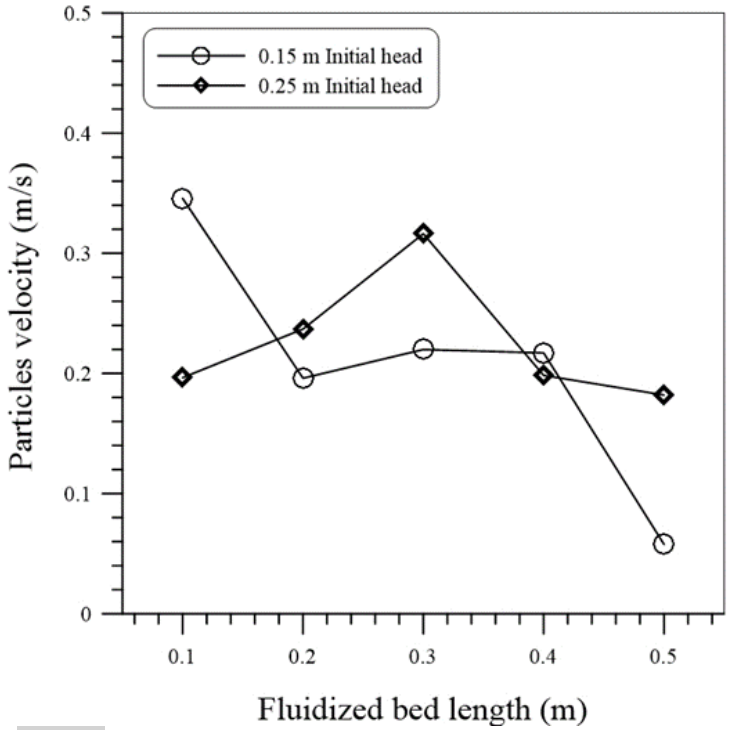

Fig. 13 Velocity of the Particles Through the Fluidized Bed.

4.CONCLUSION

Different values of water velocity were tested, as well as the initial solid particles head. It was concluded that elevating the fluidization time led to an elevation in the fluidization processes. Elevating the working fluid velocity led to an elevation in the fluidization head. Elevating the initial solid particles head led to an elevation in the fluidization head. Elevating the working fluid velocity led to an elevation in the average pressure of the fluidized bed. Elevating the initial solid particles head led to an elevation in the average pressure of the fluidized bed. Adding the wavy walls to the fluidized bed increased the mixing effect during the fluidization process. With more mixing due to the wavy walls effect, full fluidization can be reached in less time than the straight wall fluidized bed. Immersed bodies enhanced the circulation of solid particles in the fluidized bed. Also, immersed bodies reduced the average pressure inside the fluidized bed.

NOMENCLATURE

CFD	Computational fluid dynamics
g	Gravity acceleration (m/s^2)
F	Force (N)
m_{pq}, m_{qp}	Interphase mass exchange (kg/m^3.s)
Q	Flow rate of water and gasoline (l/min, m^3/s)
R_{pq}, R_{qp}	Interaction force (N)
U	Superficial velocity of water and gasoline (m/s)
Greek Symbols	
μ_q	Viscosity of the phase (kg/m. s)
α_q	Volume fraction for the phase
ε	Epsilon
ϵ	Turbulent dissipation rate (m^2/s^3)
λ_q	Bulk viscosity of the phase (kg/m. s)
v	Velocity (m/s)
ρ	Density for the phase (kg/m^3)
τ_q	Shear stress for the phase (Pa)
σ	Surface tension (kg/m)
Subscripts	
w	Water
a	Air
lift	Lift force
v_m	Virtual mass force

ACKNOWLEDGMENT

The author would like to express her profound gratitude to her department (Public Health in Veterinary Medicine College at Wasit University) for their contributions to the completion of her paper.

REFERENCES

[1] Gupta P. **Verification and Validation of a DEM-CFD Model and Multiscale Modelling of Cohesive Fluidization Regimes.** Ph.D. Thesis. University of Edinburgh; Scotland, United Kingdom: 2014.

[2] Cui Y, Fu W, Zhang Y, Cao X, Xu P, Rehan MA, Li B. **Experimental Fluidization Performances of Silicon Carbide in a Fluidized Bed.** *Chemical Engineering and Processing - Process Intensification* 2020; **154**:108016.

[3] Chokphoemphun S, Eiamsa-ard S, Promvonge P, Chuwattanakulc P. **Rice Husk Combustion Characteristics in a Rectangular Fluidized-Bed Combustor with Triple Pairs of Chevron-Shaped Discrete Ribbed Walls.** *Case Studies in Thermal Engineering* 2019; **14**:100511.

[4] Fu Z, Zhu J, Barghi S, Zhao Y, Luo Z, Duan C. **The Distribution of Bed Density in an Air Dense Medium Fluidized Bed with Single and Binary Mixtures of Geldart B and/or D Particles.** *Minerals Engineering* 2019; **142**:105926.

[5] Mandviwala C, Gonzalez-Arias J, Vilches TB, Seemann M, Thunman H. **Comparing Bed Materials for Fluidized Bed Steam Cracking of High-Density Polyethylene: Olivine, Bauxite, Silica-Sand, and Feldspar.** *Journal of Analytical and Applied Pyrolysis* 2023; **173**:106049.

[6] Oshitani J, Kato S, Tsuji T, Washino K, Harada S, Kajiwara H, Matsuoka K, Franks GF. **Influence of Air Velocity and Powder Bed Height on Local Density and Float-Sink of Spheres in a Gas-Solid Fluidized Bed.** *Advanced Powder Technology* 2023; **34**(9):104146.

[7] Liu C, Lu S, He J, Zhao Y, Zhu L. **A Modified Model for Predicting Bed Density of Air Dense Medium Gas-Solid Fluidized Bed (ADMGFB) Using Binary Dense Media.** *Powder Technology* 2019; **355**:363-371.

[8] Vodička M, Michaliková K, Hrdlička J, Hofbauer C, Winter F, Skopec P, Jeníková J. **External Bed Materials for the Oxy-Fuel Combustion of Biomass in a Bubbling Fluidized Bed.** *Journal of Cleaner Production* 2021; **321**(25): 128882.

[9] Park HC, Choi HS. **Numerical Study of the Segregation of Pyrolyzed Char in a Bubbling Fluidized Bed According to Distributor Configuration.** *Powder Technology* 2019; **355**:637-648.

[10] Zhu X, Feng X, Zou Y, Shen Y. **Effect of Baffles on Bubble Behavior in a Bubbling Fluidized Bed for Chemical Looping Processes.** *Particuology* 2020; **53**:154-167.

[11] Davarpanaha M, Shi H, Nikrityukc P, Hashisho Z. **Verification of Semi-Empirical Relations for Predicting Fluidization in a Fluidized Bed Using CFD.** *Chemical Engineering Research and Design* 2021; **173**:289-304.

[12] Ostermeier P, Fischer F, Fendt S, DeYoung S, Spliethoff H. **Coarse-Grained CFD-DEM Simulation of Biomass Gasification in a Fluidized Bed Reactor.** *Fuel* 2019; **255**(1):115790.

[13] Li J, Agarwal RK, Zhou L, Yang B. **Investigation of a Bubbling Fluidized Bed Methanation Reactor by Using CFD-DEM and Approximate Image Processing Method.** *Chemical Engineering Science* 2019; **207**(2):1107-1120.

[14] Okhovat-Alavian SM, Shabanian J, Norouzi HR, Zarghami R, Chaouki J, Mostouf N. **Effect of Interparticle Force on Gas Dynamics in a Bubbling Gas-Solid Fluidized Bed: A CFD-DEM Study.** *Chemical Engineering Research and Design* 2019; **152**:348-362.

[15] Lashaki MJ, Sarbanha AA, Movahedirad S. **Overall Particles Flow Pattern in a Two-Zone Gas Solid Fluidized Bed with a Secondary-Gas Stream.** *Chemical Engineering Research and Design* 2022; **187**:570-583.

[16] Tawfik MHM, Diab MR, Abdelmotalib HM. **Heat Transfer and Bed Dynamics Study on a Swirling**

Fluidized Bed under Various Inlet Configurations. *International Journal of Thermal Sciences* 2020; **158**:106523.

[17] Heras MD, Barreneche C, Belmonte JF, Calderón A, Fernández AI, Almendros-Ibáñez JA. **Experimental Study of Different Materials in Fluidized Beds with a Beam-Down Solar Reflector for CSP Applications.** *Solar Energy* 2020; **211**(15):683-699.

[18] Séguin MA, Hughes RW, Fitzsimmons M, Macchi A, Mehrani P. **Study of Particle Residence Time in a Pressurized Fluidized Bed with In-Bed Heat Exchanger Tubes.** *Powder Technology* 2019; **355**:201-212.

[19] Maddahi MH, Hatamipour, Jamialahmadi M. **A Model for the Prediction of Thermal Resistance of Calcium Sulfate Crystallization Fouling in a Liquid-Solid Fluidized Bed Heat Exchanger with Cylindrical Particles.** *International Journal of Thermal Sciences* 2019; **145**:106017.

[20] Jia Min Lee JM, Lim E, WC. **Heat Transfer in a Pulsating Turbulent Fluidized Bed.** *Applied Thermal Engineering* 2020; **174**(25):115321.

[21] Bardy DA, Cruickshank CA, Tezel FH, Carrier YH, Wong B. **An Experimental Investigation of Fixed and Fluidized Beds as Adsorbers in Compact Thermal Energy Storage Systems.** *Journal of Energy Storage* 2020; **31**:101648.

[22] Bai X, Yang Y, Xu Y, Feng Y, Qiu T, Wang W, He Y. **Investigation of Electrical Field Effect on the Fluidization Characteristics in a Two-Dimensional Fluidized Bed.** *Minerals Engineering* 2021; **170**(15):107035.

[23] Driessen RT, Joep JQ, Linden VD, Kersten SRA, Bos MJ, Brilman DWF. **Characterization of Mass Transfer in a Shallow Fluidized Bed for Adsorption Processes: Modeling and Supporting Experiments.** *Chemical Engineering Journal* 2020; **388**(15):123931.

[24] Errigo M, Sebastiani A, Iannello S, Materazzi M, Lettieri. **Application of Imaging Techniques for the Characterization of Lumps Behavior in Gas-Solid Fluidized Bed Reactors.** *Fuel* 2020; **349**(1):128634.

[25] Haidong Zhang, Zeneng Sun, Mengze Zhang, Yuanyuan Shao, Jesse Zhu. **Comparison of the Flow Structures and Regime Transitions Between a Cylindrical Fluidized Bed and a Square Fluidized Bed.** *Powder Technology* 2020; **376**:507-516.

[26] Munck MJAD, Peters EAJF, Kuipers JAM. **Experimental Study on Vibrating Fluidized Bed Solids Drying.** *Chemical Engineering Journal* 2023; **472**(15):144809.

[27] Ridha H, Oleiwi SH. **Numerical Investigation for Liquid-Solid Inclined Fluidized Bed.** *International Journal of Heat and Technology* 2020; **38**(1):137-144.

[28] Lv B, Deng X, Shi C, Fang C. **Effect of Agitation on Hydrodynamics and Separation Performance of Gas-Solid Separation Fluidized Bed.** *Powder Technology* 2021; **388**:129-138.

[29] Liu D, Zhang Y, Yuan Y, Grace JR. **Effect of Particle Properties on Forces on an Immersed Horizontal Slat during Start-Up of a Fluidized Bed.** *Chemical Engineering Research and Design* 2020; **159**:105-114.

[30] Fattahi M, Hosseini SH, Ahmadi G, Parvareh A. **Numerical Simulation of Heat Transfer Coefficient around Different Immersed Bodies in a Fluidized Bed Containing Geldart B Particles.** *International Journal of Heat and Mass Transfer* 2019; **141**:353-366.

[31] Al-Turaihi RS, Oleiwi SH. **Experimental and CFD Investigation the Effect of Solid Particle Height in Water-Solid Flow in Fluidized Bed Column.** *International Journal of Mechanical Engineering and Applications* 2015; **3**(3):37-45.

[32] Hessels CJM, Lelivelt DWJ, Stevens NC, Tang YY, Deen NG, Finotello G. **Minimum Fluidization Velocity and Reduction Behavior of Combusted Iron Powder in a Fluidized Bed.** *Fuel* 2023; **342**(15):127710.

[33] Córcoles JI, Iborra AA, Ibáñez JAA. **Influence of Immersed Surface Shape on the Heat Transfer Process and Flow Pattern in a Fluidized Bed Using Numerical Simulation.** *International Journal of Heat and Mass Transfer* 2021; **178**:121621.

[34] Dai L, Yuan Z. **Characteristics of Geldart-B Particles in Fluidized Beds.** *5th World Congress on Mechanical, Chemical and Material Engineering* 2019 August 15-17; Lisbon, Portugal: HTFF 125-1-HTFF 125-5.

[35] Gosavi S, Kulkarni N, Mathpati CS, Manda D. **CFD Modeling to Determine the Minimum Fluidization Velocity of Particles in Gas-Solid Fluidized Bed at Different Temperature.** *Powder Technology* 2017; **327**:109-119.

[36] Yingjuan S, Jinrao G, Zhong W, Yu A. **Determination of Minimum Fluidization Velocity in Fluidized**

Bed at Elevated Pressures and Temperatures Using CFD Simulations. *Powder Technology* 2019; **350**(5):81-90.

[37] Abbas EF, Izat BS. **Effect of Fluidized Bed Particle Size on Heat Transfer Coefficient at Different Operating Conditions.** *Tikrit Journal of Engineering Sciences* 2018; **25**(4):24-29.